The Astronomical Journal, 136:1519–1522, 2008 October doi:10.1088/0004-6256/136/4/1519

LONG-WAVELENGTH DENSITY FLUCTUATIONS RESOLVED IN PLUTO'S HIGH ATMOSPHERE

D. W. McCarthy[1], W. B. Hubbard[2], C. A. Kulesa[1], S. D. Benecchi[3], M. J. Person[4], J. L. Elliot[4,5], and A. A. S. Gulbis[4,6]
[1] Steward Observatory, University of Arizona, 933 N. Cherry Ave, Tucson, AZ 85721, USA; dmccarthy@as.arizona.edu
[2] Lunar and Planetary Laboratory, University of Arizona, 1629 E. University Blvd., Tucson, AZ 85721, USA
[3] Space Telescope Science Institute, 3700 San Martin Drive, Baltimore, MD 21218, USA
[4] Earth, Atmospheric and Planetary Sciences, MIT, 77 Massachusetts Ave., Cambridge, MA 02139, USA
[5] Department of Physics, MIT, 77 Massachusetts Ave., Cambridge, MA 02139, USA
[6] South African Astronomical Observatory, P.O. Box 9, Observatory, 7935 Cape Town, South Africa
Received 2008 May 16; accepted 2008 July 22; published 2008 September 8

ABSTRACT

Near-infrared measurements of the occultation of star P445.3 by Pluto on 2007 March 18 reveal that Pluto's upper atmosphere (∼200–400 km altitude) is unexpectedly dynamic. At a wavelength of 1.6 μm, numerous vertical fluctuations (8–20 km) of density are detected with unprecedented signal-to-noise ratio. These fluctuations are achromatic, nearly limb-aligned, and fully resolved along a ∼1000 km path over a pressure range of ∼0.1–0.7 μbar (0.01 to 0.07 Pa). Vertical wavelength increases with altitude indicating a high-frequency cutoff operating on a broad-band spectrum of buoyancy ("gravity") waves generated deeper in Pluto's atmosphere.

Key words: Kuiper Belt – occultations – planets and satellites: individual (Pluto)

1. INTRODUCTION

Despite the tenuous nature of Pluto's atmosphere (surface pressure ∼30 μbar), stellar occultations can be used to measure the profile of physical characteristics versus altitude and also to monitor temporal changes as Pluto continues to recede from perihelion. Previous studies have suggested the presence of near-surface haze layers and indicated that increasing atmospheric pressure (Elliot et al. 2003, 2007) may be caused by frost migration (Hansen & Paige 1996). In order to detect extinction caused by low-lying haze and to continue monitoring Pluto's atmosphere in preparation for the flyby mission of *New Horizons*, we conducted dual-wavelength observations of the occultation of star P445.3 by Pluto on 2007 March 18 (UT). This paper presents the near-infrared results at 1.6 μm. A companion paper by Person et al. (2008) describes the visible results as well as the astrometric solution derived from light curves at five sites.

2. OBSERVATIONS

The occultation of star P445.3 (2UCAC 25823784) by Pluto was observed in both near-infrared and visible wavelengths on 2007 March 18 (UT) at the 6.5 m MMT on Mt. Hopkins. The primary camera, PISCES (McCarthy et al. 2001), recorded the event in the *H*-band (1.6 μm) using 80 × 80 pixel frames (14.4 arcsec on a side) at a rate of 2.5 Hz with a duty cycle of 70%. Despite a relatively low elevation angle (∼20°) and high air mass (∼3), individual frames display signal-to-noise ratio (S/N) ∼100 and resolve Pluto and Charon (separation 0.719 ± 0.008 arcsec; $\Delta m = 1.94 \pm 0.03$ mag). A dichroic beam splitter located immediately above PISCES reflected visible light (<1 μm) into the f/9 Top Box where the beam was collimated and reimaged onto a secondary camera (Souza et al. 2006; Person et al. 2008) recording with an effective wavelength of 0.75 μm at 4 Hz. The 1.6 μm measurements were obtained continuously from 9:56 to 11:30 UTC, and no drop in signal (<0.5%) was observed during Charon's orbital crossing within ±2.5 min of 10:20 UTC.

3. DISCUSSION

3.1. Detection of Light Curve Fluctuations

Figure 1 shows the 1.6 μm light curve compared with a reference theoretical light curve for a simple pure-nitrogen atmosphere at constant temperature and pressure ($T = 100$ K, $P = 30$ μbar at 1150 km radius). This model atmosphere provides a smooth reference for analyzing the numerous fluctuations recorded throughout the occultation event. Since these fluctuations were not detected in a reference star recorded simultaneously in the same field of view at a separation of ∼6 arcsec, they are clearly associated with Pluto. The isothermal model does not constrain the true surface pressure because these data give no information about atmospheric radii less than about 1348 km.

Based on a study of additional observations of this occultation (Person et al. 2008), we use values for the Mt. Hopkins impact parameter to the shadow center (1319 ± 4 km) and shadow-plane speed (6.77 km s^{-1}) and take the time of closest approach to be 10:30:00 UTC + 1428.26 ± 0.25 s. The isothermal model has a minimum relative stellar flux at midoccultation equal to 0.69. The corresponding minimum closest approach distance for the primary ray is 1348 km from Pluto's center.

The unusually slow shadow speed for this event, together with unprecedented S/N at 1.6 μm and the grazing geometry for the occultation, permits us to perform a detailed investigation of the prominent, well-sampled fluctuations visible in the data. These fluctuations span a pressure range of ∼0.1–0.7 μbar (0.01 to 0.07 Pa) corresponding to an altitude range of 1500–1350 km, respectively.

The bottom portion of Figure 1 shows that the residuals between the *H*-band and somewhat noisier *V*-band (Person et al. 2008) data are indistinguishable from the small predicted color difference due to dispersion in Pluto's nitrogen atmosphere. Therefore, there are no detectable chromatic effects in the two-wavelength data set, and no haze layers were detected over this altitude range. The refractivity of nitrogen gas increases by 0.8% from the *H*-band to the visible band (Bennett 1934), implying a maximum occultation depth difference due to differential refraction of 0.18% for this event.

The absence of chromatic effects is consistent with the spatial width of the fluctuations in the data, which is always in excess of 5 km along the occultation chord. The Fresnel scale for this occultation was 1.8 km at 0.75 μm and 3.2 km at 1.6 μm, significantly greater than the projected diameter (∼0.7 km) of an MIII-type star implied by infrared photometry (Skrutskie et al.

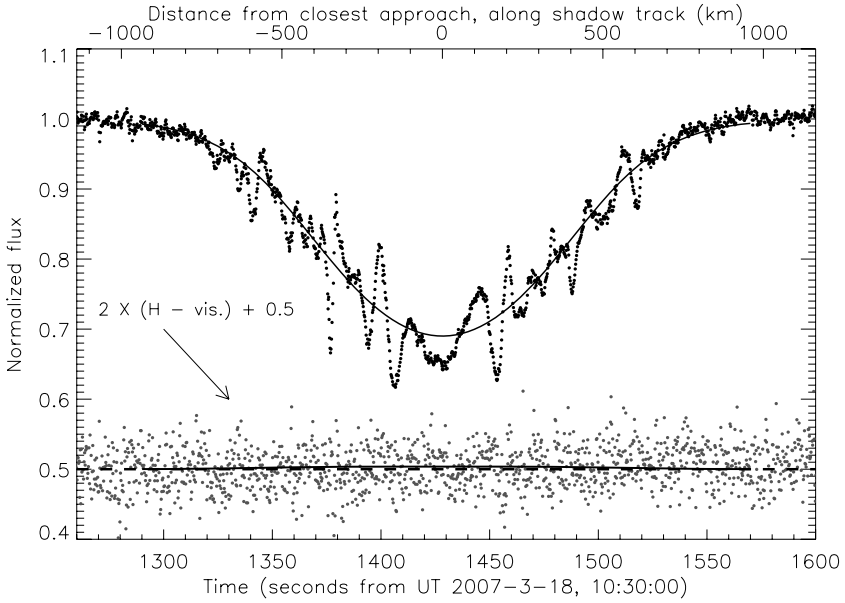

Figure 1. Stellar flux vs. time at 1.6 μm. Flux is normalized to unity outside of occultation and compared with a reference theoretical light curve for pure nitrogen, isothermal Pluto atmosphere (smooth curve). The lower plot shows the residuals between the normalized *H*-band and normalized visible-wavelength (Person et al. 2008) data. For ease of display these residuals were shifted upward by 0.5 and magnified by a factor of 2 with respect to the *H*-band light curve. A horizontal dashed line corresponded to zero and the smooth line, slightly bowed upward with respect to the dashed line, and almost invisible at this scale, shows the small predicted color difference due to dispersion in Pluto's nitrogen atmosphere.

2006). Therefore, the fluctuations are not the diffractive scintillations ("spikes") frequently observed in planetary occultations or the twinkling of stars in the Earth's atmosphere (Hubbard et al. 1988). Because of the unusual grazing geometry of the present event, the fluctuations are amenable to interpretation using weak-scintillation theory (Hubbard et al. 1978). This theory is applied to our data in W. B. Hubbard et al. (2008, in preparation). Here we emphasize a robust, essentially theory-independent result from our initial data analysis: the long wavelength nature of the density fluctuations suggests that a physical mechanism filters out shorter wavelength fluctuations with increasing altitude in Pluto's atmosphere.

The fluctuations show some degree of symmetry about mid-occultation, but the symmetry is not perfect. Figure 2 shows the *H*-band light curve fluctuations plotted as a function of the closest-approach distance of the ray from the center of Pluto, assuming the geometric parameters of the isothermal model. The fluctuations in the immersion and emersion segments of the light curve show some symmetry about the closest-approach point but are typically misaligned by ∼1–5 km. This result implies that atmospheric density fluctuations giving rise to the light curve fluctuations are not strictly a function of radius but are inclined to the limb by angles $\sim 10^{-2}$ radians.

3.2. Gravity Wave Interpretation

The theory that we apply (W. B. Hubbard et al. 2008, in preparation) makes the following approximations: we neglect any background winds, assume that the unperturbed atmosphere has a constant scale height $H \sim 60$ km (corresponding to an average temperature $\bar{T} = 100$ K), and assume a plane-parallel atmosphere (i.e., we ignore sphericity). We focus on inertia-gravity waves, although Rossby waves, as suggested by Person et al. (2008), may also be present in the data. Following Fritts (1984), we consider a wave in two dimensions, varying in x (parallel to the limb) and z (perpendicular to the limb). The corresponding spatial wavenumbers are k in the x-direction and m in the z-direction. For gravity waves, wavenumbers and

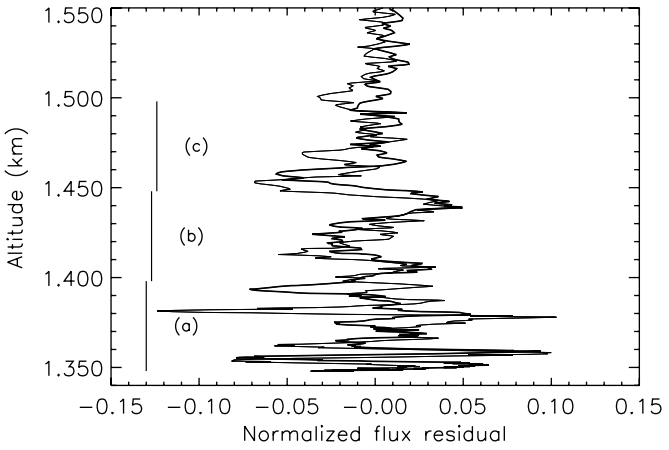

Figure 2. Fluctuations in the normalized flux, $\Delta\phi$, vs. radius of ray closest approach to Pluto (thin curves are for data prior to midoccultation and heavy curves after midoccultation). Vertical bars labeled (a), (b), (c) show altitude intervals in which power spectra were obtained for the fluctuations. Those spectra are shown in Figure 3.

frequency ω are related by the dispersion relation (French & Gierasch 1974)

$$\omega^2 = \frac{\omega_B^2 k^2 + f^2 m^2}{k^2 + m^2}, \quad (1)$$

where f is the Coriolis frequency and ω_B is the Brunt–Väisälä frequency for an isothermal atmosphere at temperature $\bar{T}$, given by

$$\omega_B^2 = \frac{\gamma - 1}{\gamma}\frac{g}{H} = \frac{g^2}{C_P \bar{T}}, \quad (2)$$

where $g = 45$ cm s^{-2} is Pluto's average gravity in the range considered here, C_p is the heat capacity at constant pressure, and for N_2 gas $\gamma = 1.4$.

In the case of the present observation, we observe waves with $k^2 \ll m^2$, because the occultation geometry averages

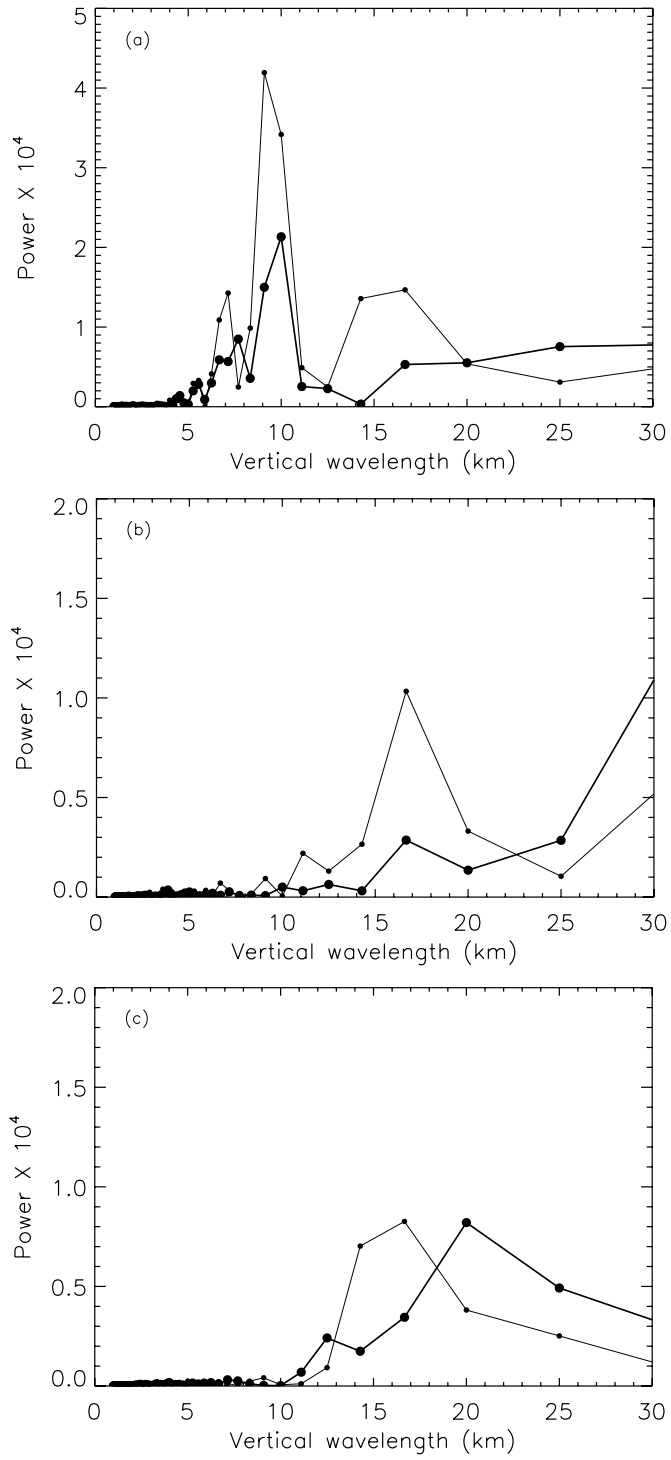

Figure 3. (a) Power spectrum (in wavenumber m) vs. vertical wavelength $\lambda_z = 2\pi/m$, for altitude interval (a) from 1350 to 1400 km. The thin curves are for data prior to midoccultation and heavy curves after midoccultation. (b) Power spectrum (in wavenumber m) vs. wavelength, for altitude interval (b) from 1400 to 1450 km. (c) Power spectrum (in wavenumber m) vs. wavelength, for altitude interval (c) from 1450 to 1500 km.

out atmospheric disturbances over an effective path length $\ell \approx 2\sqrt{2rH} \approx 1000$ km, where $r \sim 1400$ km. We adopt $k \sim 2\pi/1000$ km^{-1}, whereas $m \sim 2\pi/10$ km^{-1}. We adopt $\omega_B = 1.44 \times 10^{-3}$ s^{-1} and $f \sim 2 \times 10^{-5}$ s^{-1}. Since $f/\omega_B \sim 0.01$, dispersion relation (1) reduces to

$$m^2 \approx \frac{k^2\omega_B^2}{\omega^2 - f^2}. \tag{3}$$

Define

$$\nabla = \frac{d\ln T}{d\ln P}. \tag{4}$$

Using Houghton's (1977) Equations (8.16)–(8.19), one can show that

$$\frac{(P'/\bar{P})}{(\rho'/\bar{\rho})} = -\frac{1}{Hm}, \tag{5}$$

where P' is the gravity wave's pressure perturbation to the local pressure $\bar{P}$ of the background isothermal atmosphere, and ρ' is the mass density perturbation to the background density $\bar{\rho}$. For an ideal gas, we have

$$\frac{T'}{\bar{T}} = \frac{P'}{\bar{P}} - \frac{\rho'}{\bar{\rho}} = \frac{P'}{\bar{P}}(1 + Hm), \tag{6}$$

so

$$\nabla = H^2m^2\frac{P'}{\bar{P}} = -Hm\frac{\rho'}{\bar{\rho}}. \tag{7}$$

A gravity wave with vertical wavenumber m breaks when $|\nabla| > (\gamma - 1)/\gamma$, or when

$$(\rho'/\bar{\rho}) \approx \frac{\gamma - 1}{\gamma}\frac{1}{Hm}. \tag{8}$$

Equation (8) predicts a density amplitude (relative to the reference density profile) equal to 0.006 for $\lambda_z = 8$ km and 0.015 for $\lambda_z = 20$ km. The relative density fluctuations inferred from our data and the visual-band data (Person et al. 2008) are suggestively close to these values, which may support the hypothesis that the observed fluctuations are produced by nearly-breaking gravity waves high in Pluto's atmosphere. If the long-wavelength fluctuations that we observe are indeed gravity waves, Equation (3) implies that their frequencies are close to f, which will provide a further constraint on the gravity-wave interpretation (W. B. Hubbard et al. 2008, in preparation).

Liller & Whipple's (1954; pp. 112–130) observations of meteor trails were among the first detections of breaking gravity waves in the Earth's atmosphere at heights of ~80 km to ~115 km (pressures similar to those investigated here). Over a few hours, the meteor trails became distorted by mainly horizontal winds, over vertical scales ~5–15 km. The wind velocities and vertical distortion scales were observed to increase with height. The density fluctuations that we have observed in Pluto's atmosphere resemble this phenomenon.

The results reported here demonstrate the effectiveness of high S/N occultation measurements made possible with a large aperture telescope and a sensitive camera. The density fluctuations which we have detected correspond to bending angles of $\sim 5 \times 10^{-11}$ radians in the refraction of starlight. Stellar occultation is the only technique capable of reaching such precision. In contrast, the radio-occultation experiment on *New Horizons* can detect refractive bending angles of $\sim 10^{-8}$ radians (Tyler et al. 2008). As Pluto's location heads into the galactic plane, new stellar-occultation opportunities are expected to arise (McDonald & Elliot 2000) and should be explored to further

characterize and monitor the dynamics of Pluto's atmosphere before *New Horizons* arrives in the year 2015.

Observations reported here were obtained at the MMT Observatory, a joint facility of The University of Arizona and the Smithsonian Institution. We acknowledge the extensive engineering support of the entire MMTO staff, especially Mr. Shawn Callahan. The integration and alignment of both cameras was funded by the Astronomy Camp science education program.This publication makes use of data products from the Two Micron All Sky Survey, which is a joint project of the University of Massachusetts and the Infrared Processing and Analysis Center/California Institute of Technology, funded by the National Aeronautics and Space Administration and the National Science Foundation. We are grateful for the positive contributions and suggestions provided by the anonymous referee. Drs. S.D.B., J.L.E., A.A.S.G., and M.J.P. acknowledge support from NASA's Planetary Astronomy Program via grants NNG04GE48G and NNG04GF25G.

REFERENCES

Bennett, C. E. 1934, Phys. Rev., 45, 200
Elliot, J., et al. 2003, Nature, 424, 165
Elliott, J., et al. 2007, AJ, 134, 1
French, R. G., & Gierasch, P. J. 1974, J. Atmos. Sci., 31, 1707
Fritts, D. C. 1984, Rev. Geophys. Space Phys., 22, 275
Hansen, C. J., & Paige, D. A. 1996, Icarus, 120, 247
Houghton, J. T. 1977, The Physics of Atmospheres (Cambridge: Cambridge Univ. Press), Chapter 8
Hubbard, W. B., Jokipii, J. R., & Wilking, B. A. 1978, Icarus, 34, 374
Hubbard, W. B., Lellouch, E., Sicardy, B., Brahic, A., Vilas, F., Bouchet, P., McLaren, R. A., & Perrier, C. 1988, AJ, 325, 490
Liller, W., & Whipple, F. 1954, Rocket Exploration of the Upper Atmosphere (Oxford: Pergamon Press Ltd.)
McCarthy, D., Ge, J., Hinz, J., Finn, R., & de Jong, R. 2001, PASP, 115, 353
McDonald, S. W., & Elliot, J. L. 2000, AJ, 119, 1999
Person, M., et al. 2008, AJ, 136, 1510
Skrutskie, M. F., et al. 2006, AJ, 131, 1163
Souza, S., et al. 2006, PASP, 118, 1550
Tyler, G. L., et al. 2008, Space Sci. Rev., http://dx.doi.org/10.1007/s11214-007-9302-3